

# Long-Range Dependence in Financial Markets: a Moving Average Cluster Entropy approach

Pietro Murialdo<sup>1</sup> Linda Ponta<sup>2</sup>, Anna Carbone<sup>1</sup>,

**1** Politecnico di Torino, corso Duca degli Abruzzi 24, 10129 Torino, Italy

**2** LIUC-Università Cattaneo, corso Giacomo Matteotti 22, 21053 Castellanza, Italy

## Abstract

A perspective is taken on the intangible complexity of economic and social systems by investigating the underlying dynamical processes that produce, store and transmit information in financial time series in terms of the *moving average cluster entropy*. An extensive analysis has evidenced market and horizon dependence of the *moving average cluster entropy* in real world financial assets. The origin of the behavior is scrutinized by applying the *moving average cluster entropy* approach to long-range correlated stochastic processes as the Autoregressive Fractionally Integrated Moving Average (ARFIMA) and Fractional Brownian motion (FBM). To that end, an extensive set of series is generated with a broad range of values of the Hurst exponent  $H$  and of the autoregressive, differencing and moving average parameters  $p, d, q$ . A systematic relation between *moving average cluster entropy*, *Market Dynamic Index* and long-range correlation parameters  $H, d$  is observed. This study shows that the characteristic behaviour exhibited by the horizon dependence of the cluster entropy is related to long-range positive correlation in financial markets. Specifically, long range positively correlated ARFIMA processes with differencing parameter  $d \simeq 0.05$ ,  $d \simeq 0.15$  and  $d \simeq 0.25$  are consistent with *moving average cluster entropy* results obtained in time series of DJIA, S&P500 and NASDAQ.

## 1 Introduction

In recent years, much effort has been spent on studying complex interactions in financial markets by means of information theoretical measures from different standpoints. The information flow can be probed by observing a relevant quantity over a certain temporal range (e.g. price and volatility series of financial assets).

Socio-economic complex systems exhibit remarkable features related to patterns emerging from the seemingly random structure in the observed time series, due to the interplay of long- and short-range correlated decay processes. The correlation degree is intrinsically linked to the information embedded in the patterns, whose extraction and quantification allow one to add clues to the underlying complex phenomena [1–15].

An information measure  $S(x)$  was proposed by Claude Shannon to the aim of quantifying the degree of uncertainty of strings of elementary random events in terms of their probabilities [16]. The elementary stochastic events are related to a relevant variable  $x$  whose values are determined by the probability  $\{p_i\}$ . For example, the size  $\ell$  of a string (block), corresponding to a particular realization within the sequence, can be associated to the probability  $p_i(\ell)$  that, for stationary processes, does not depend on

the actual position of the string (block) in the sequence. The Shannon measure is then given by the expectation value of every possible event  $S(\ell) = \sum_i p_i(\ell) \log p_i(\ell)$ . The Shannon entropy is calculated over all possible strings and the entropy density  $s_\ell = \lim_{\ell \rightarrow \infty} S(\ell)/\ell$  quantifies the rate at which the process produces unexpected information as a function of the size  $\ell$ .

A complexity measure  $K(x)$  was proposed by Kolmogorov to quantify the amount of information contained in the string  $x$  [17]. The relation between Kolmogorov complexity and Shannon entropy has been extensively investigated in [18]. The entropy density  $s_\ell$  for a stationary process is equal to the Kolmogorov entropy rate.

The first step required for the practical implementation of entropy and complexity measures is a suitable partition of the sequence which is critical to unbundle random and deterministic blocks of given length (decryption). The method usually adopted for partitioning a sequence and estimating its entropy is based on a uniform division in blocks with same length [19–22].

The *cluster entropy method* [10–12] implements the partition via a moving average process. The *clusters* correspond to blocks of different sizes, defined as the portion between consecutive intersections of a given time series and moving average. The *cluster entropy method* has been applied to financial markets in [23, 24]. Cumulative information measures (indexes) have been worked out with the ability to provide deep insights on heterogeneity and dynamics. In particular:

- **Heterogeneity.** Volatility series have been analysed by using the cluster entropy approach over constant temporal horizon (six years of tick-by-tick data sampled every minute). An information measure of heterogeneity, the *Market Heterogeneity Index*  $I(T, n)$ , where  $T$  and  $n$  are respectively the volatility and moving average windows, has been developed by integrating the cluster entropy curves of the volatility series over the cluster length  $\tau$ . It has been also shown that the *Market Heterogeneity Index* can be used to yield the weights of an efficient portfolio as a complement to Markowitz and Sharpe traditional approaches for markets not consistent with Gaussian conditions [23].
- **Dynamics.** Prices series have been investigated by using the cluster entropy approach over several temporal horizons (ranging from one to twelve months of tick-by-tick data with sampling interval between 1 up to 20 seconds depending on the specific market). The study has revealed a systematic dependence of the cluster entropy over time horizons in the investigated markets. The *Market Dynamic Index*  $I(M, n)$ , where  $M$  is the temporal horizon and  $n$  is the moving average window, defined as the integral of the cluster entropy over  $\tau$ , demonstrates its ability to quantify the dynamics of assets' prices over consecutive time periods in a single figure [24].

The present study is motivated by the results obtained in [24] showing that cluster entropy of real-world financial markets (NASDAQ, DJIA and S&P500) exhibits significant *market and horizon dependence*. According to classical financial theories, subsequent price deviations are identically and independently distributed (*iid*). All the information would be immediately reflected into markets, thus hampering past observations to predict future outcomes. If that were true, correlation would be negligible and prices would be simply modelled in terms of *fully uncorrelated Brownian motion*. However, several studies have shown that real world markets only partially behave according to the standard theory of perfectly informed and rational agents.

Here, we add further clues to the microscopic origin of the horizon dependence of the cluster entropy in financial markets. To this purpose, the cluster entropy approach is applied to an extensive set of artificially generated series with the aim of shedding light on the characteristic behaviour of real world assets [24]. We report results of the cluster

entropy in *Geometric Brownian Motion* (GBM), *Fractional Brownian Motion* (FBM) and *Autoregressive Fractionally Integrated Moving Average* (ARFIMA) processes. Those are well-known processes characterized either by hyperbolically decaying or exponentially decaying correlation functions, features reflected in long-range or short-range dependent dynamics of the elementary random events. The performance of the *Autoregressive Fractionally Integrated Moving Average* (ARFIMA) process and its variants are receiving a lot of attention and are under intense investigation in the financial research community [25–29]. This work clearly demonstrates the relationship between the endogenous dynamics of the time series and their long-range dependence.

It is shown that deviations of the moving average cluster entropy behaviour in comparison to simple Brownian motion is unequivocally related to the long-range dependence of real-world market series. In particular, moving average cluster entropy results obtained on Fractional Brownian Motion with Hurst exponent  $H$  in the range  $0 \leq H \leq 0.5$  (negatively correlated series) show no time horizon dependence. Conversely cluster entropy curves with Hurst exponent  $H$  in the range  $0.5 \leq H \leq 1$  (positively correlated series) exhibit some dispersion in the horizon dependence in analogy with the real-world financial markets. Results obtained on ARFIMA series confirm and extend the findings reported for FBMs. Horizon dependence of the cluster entropy is observed for a differencing parameter  $0 \leq d \leq 0.5$ . Fine tuning of the horizon dependence is obtained by varying the autoregressive  $p$  and moving average  $q$  components in the ARFIMA series.

The organisation of the work is as follows. The cluster entropy method used for the analysis and the investigated market and artificial data are described in Section 2. Results on cluster entropy and market dynamic index estimated over *Geometric Brownian Motion* (GBM), *Fractional Brownian Motion* (FBM) and *Autoregressive Fractionally Integrated Moving Average* (ARFIMA) series, are reported in Section 3. Finally, results are discussed, conclusions are drawn and a path for future work is suggested in Section 4.

## 2 Methods and Data

In this section the cluster entropy approach developed in [10,11] is briefly recalled. The second part of this section is devoted to the description of financial market data used in [24]. For the sake of completeness, we also recall the main definitions related to the Fractional Brownian Motion and Autoregressive Fractionally Integrated Moving Average processes.

### 2.1 Cluster Entropy Method

It is well-known that the general idea behind Shannon entropy is to measure the amount of information embedded in a message to identify the shortest subsequence actually carrying the relevant information and the degree of redundancy which is not necessary to reproduce the initial message. The Shannon functional is written as:

$$S(\tau, n) = \sum P(\tau, n) \log P(\tau, n), \quad (1)$$

where  $P(\tau, n)$  is a probability distribution associated with the time series  $y(t)$ . To the aim of estimating the probability distribution  $P(\tau, n)$ , it is necessary to partition the continuous phase space into disjoint sets. The traditionally adopted methods divide the sequence into segments of equal lengths (blocks). Here, we follow another approach.

In [10, 11] the time sequence  $y(t)$ , is partitioned in *clusters* by the intersection with its moving average  $\tilde{y}_n(t)$ , with  $n$  the size of the moving average. The simplest type of

moving average is defined at each  $t$  as the average of the  $n$  past observation from  $t$  to  $t - n + 1$ ,

$$\tilde{y}_n(t) = \frac{1}{n} \sum_{k=0}^{n-1} y(t-k). \quad (2)$$

Note that while the original series is defined from 1 to  $N$ , the moving average series is defined from 1 to  $N - n + 1$  because  $n$  samples are necessary to initialize the series. The original series and the moving average series are indicated as  $\{y(t)\}_{t=1}^N$  and  $\{\tilde{y}_n(t)\}_{t=1}^{N-n+1}$  respectively. Consecutive intersections of the time series and of the moving average series yield a partition of the phase space into a series of *clusters*. Each cluster is defined as the portion of the time series  $y(t)$  between two consecutive intersection of  $y(t)$  itself and its moving average  $\tilde{y}_n(t)$  and has length (or duration) equal to:

$$\tau_j \equiv ||t_j - t_{j-1}||, \quad (3)$$

where  $t_{j-1}$  and  $t_j$  refers to two subsequent intersections of  $y(t)$  and  $\tilde{y}_n(t)$ . For each moving average window  $n$  the probability distribution function  $P(\tau, n)$  which associates the length of a cluster  $\tau$  with its frequency can be obtained by counting the number of clusters  $\mathcal{N}_j(\tau_j, n)$  with length  $\tau_j$ ,  $j \in \{1, N - n - 1\}$ . The probability distribution function  $P(\tau, n)$  results:

$$P(\tau, n) \sim \tau^{-D} \mathcal{F}(\tau, n) \quad , \quad (4)$$

where  $D = 2 - H$  indicates the fractal dimension with  $H$  the Hurst exponent of the sequence. In this framework long-range correlation implies that the clusters are organized in a similar way along the time series (self-organized), even for clusters far away in time from each other. The term  $\mathcal{F}(\tau, n)$  in Equation (4) takes the form:

$$\mathcal{F}(\tau, n) \equiv e^{-\tau/n} \quad , \quad (5)$$

to account for the drop-off of the power-law behavior for  $\tau < n$  and the onset of the exponential decay when  $\tau \geq n$  due to the finiteness of  $n$ . When  $n \rightarrow 1$  the lengths  $\tau$  of clusters tend to be centered around a single value. When  $n \rightarrow N$ , that is when  $n$  tends to the length of the whole sequence, only one cluster with  $\tau = N$  is generated. For middle values of  $n$  however a broader range of lengths is obtained and therefore the probability distribution spreads all values. When the probability distribution in Eq. (4) is fed into the Shannon functional in Eq. (1) the result is the following:

$$S(\tau, n) = S_0 + \log \tau^D - \log \mathcal{F}(\tau, n), \quad (6)$$

which, after substituting Eq. (5), becomes:

$$S(\tau, n) = S_0 + \log \tau^D + \frac{\tau}{n}, \quad (7)$$

where  $S_0$  is a constant,  $\log \tau^D$  accounts for power-law correlated clusters related to  $\tau^{-D}$  and  $\tau/n$  accounts for exponentially correlated clusters related to the term  $\mathcal{F}(\tau, n)$ . The term  $S_0$  can be evaluated in the limit  $\tau \sim n \rightarrow 1$ , which results in  $S_0 \rightarrow -1$  and  $S(\tau, n) \rightarrow 0$ , that corresponds to the fully deterministic case, where each cluster has size equal to 1. On the other hand, when  $\tau \sim n \rightarrow N$ , the maximum value for the entropy is obtained with  $S(\tau, n) = \log N^D$ , which corresponds to the case of maximum randomness, where there is one cluster coinciding with the whole series. Equation (7) shows that power-law correlated clusters, characterized by having length  $\tau < n$ , are described by a logarithmic term as  $\log \tau^D$ , and their entropy do not depend on the moving average window  $n$ . However, for values of  $\tau \geq n$ , which represent exponentially correlated clusters, the term  $\tau/n$  becomes predominant. Cluster entropy increases

linearly as  $\tau/n$ , with slope decreasing as  $1/n$ . Hence, due to the finite size effects introduced by the partitioning method, in  $\tau = n$  the behavior of entropy changes and its values exceeds the curve  $\log \tau^D$ . In other words, clusters that are power-law correlated does not depend on  $n$ , are said to be *ordered* and represent deterministic information. Clusters that are exponentially correlated does depend on  $n$ , are said to be *disordered* and represent random clusters.

The meaning of entropy in information theory can be compared with the meaning of entropy in thermodynamics. In an *isolated system*, the entropy increase  $dS$  refers to the irreversible processes occurring spontaneously within the system. In an *open system* however a further increase in entropy  $dS_{ext}$  occurs due to the irreversible processes spontaneously occurring with the external environment.

The term  $\log \tau^D$  should be interpreted as the entropy of the isolated system. It is independent on  $n$ , that is it is independent on the partitioning method. It takes the form of the Boltzmann entropy, that can be written as  $S = \log \Omega$ , with  $\Omega$  the volume of the system. Therefore the quantity  $\tau^D$  corresponds to the volume occupied by the fractional random walker.

The term  $\tau/n$  represents the excess entropy caused by the external process of partitioning the sequence. The excess entropy depends on the moving average window  $n$ . If same size boxes were chosen, the excess entropy term  $\tau/n$  would vanish and entropy would reduce to the logarithmic term. When a moving average partition is used, the term  $\tau/n$  emerges to account for the additional heterogeneity introduced by the randomness of the process. Thence, for exponentially correlated clusters entropy exceeds the logarithmic asymptotic.

One important step is to quantify the property of the entropy result. In order to improve the accuracy of the method, one can consider the integral of the entropy function over the clusters length  $\tau$ , a cumulative measure able to embed all information in a single figure:

$$I(n) = \int S(\tau, n) d\tau \quad , \quad (8)$$

which for discrete sets reduces to  $I(n) = \sum_{\tau} S(\tau, n)$ . Eq. (8) can be written as:

$$I(n) = \int_1^{\tau(n)} S(\tau, n) d\tau + \int_{\tau(n)}^{\infty} S(\tau, n) d\tau \quad . \quad (9)$$

The first integration is referred to the power law regime of the cluster entropy, the second integration is referred to the linear regime of the cluster entropy (i.e. the excess entropy term).

## 2.2 Data

### 2.2.1 Financial Data

The objective of this work is to investigate and shed light on the characteristic features exhibited by cluster entropy of financial markets. In particular here our focus is on the systematic dependence of the cluster entropy of the price series over time horizon  $M$ .

In [24] the cluster entropy is applied to a large set of tick-by-tick data of the USA's indexes (S&P500, NASDAQ and DJIA). NASDAQ is an index resulting from all the public firms quoted on the market, DJIA and S&P500 indexes are representative of a selected number of public firms. For each index, investigated data include tick-by-tick prices from January 2018 to December 2018. More information about the markets can be found at the Bloomberg terminal.

To study the dynamics of financial series different time horizons need to be compared. As explained in the Introduction, entropy is sample-size dependent by definition, thus in

order to rule out spurious results the length of the investigated sequences must be the same. Therefore, cluster entropy analysis requires the comparison to be implemented on series with same length. Raw data have been downloaded from the Bloomberg terminal in the form of tick-by-tick data. The lengths of the raw series vary due to different number of trading days and transactions per time unit. It is therefore necessary, as first computational step, to implement a sampling of the raw data to make the length of the series exactly the same. The first raw series ranges from the first transaction of January 2018 to the last one of January 2018; the second ranges from the first transaction in January 2018 to the last of February 2018, ..., the twelfth ranges from the first transaction in January 2018 to the last of December 2018, a period equivalent to the whole year. Because each raw series ranges from the first tick of 2018 to the last tick of the relative month, the twelve series have very different lengths. The series are sampled to obtain twelve *series* with same length as described in the following.

Twelve sampling time intervals and corresponding frequencies must be defined, i.e. twelve integers indicating for each series the interval of skipped data. Sampling intervals are obtained by dividing the length of each raw series by the length of the shortest raw one and then rounding to the inferior integer. Thence, each raw series is sampled with the relative sampling interval to yield a *sampled series*: for each sample in the sampled series, a number of samples equal to the sampling frequency has been discarded in the raw series. The sampled series obtained are *approximately* of equal lengths. To obtain twelve series of *exactly* equal length, a few observations are cut off, when exceeding the length of the shortest series. The result consists in twelve sampled series that are equal in length and refer to time horizons varying from one month ( $M = 1$ ) to twelve months ( $M = 12$ ). In more details, the length of the series corresponding to the  $M$  different horizons is  $N_M$  (where  $M$  ranges from 1 to 12 for one year of data). Among the monthly series, the shortest month is used to evaluate the minimum value of  $N_{min}$  and, correspondingly, of the sampling frequency. Then, the sampling intervals for the multiple periods is derived by dividing the multiple period lengths (i.e. the sum of multiple consecutive  $N_M$ ) by the value  $N_{min}$ . In Table 1 a few examples of sampling intervals and lengths  $N_M$  are shown for clarify the procedure. It is worth noting that the length of sampled series should be at least  $10^5$  to ensure enough accuracy of the results.

## 2.3 Artificial Data

Artificial series have been generated by using FBM and ARFIMA processes with same temporal structure corresponding to the different horizons of the financial market data reported in [24]. Artificial series were generated with length equal to those of the twelfth cumulative series analysed in [24]. Thence, we divided the series in the respective cumulative series according to the lengths obtained for NASDAQ cumulative series reported in [24]. Then the sampling method proceeds analogously from the calculation of the sampling frequency. Such sampling method was applied to series generated by artificial financial models to make sure that the information content would be comparable to that of real-world financial series. In the remainder of this section, we recall the main definitions for Fractional Brownian Motion and Autoregressive Fractionally Integrated Moving Average processes.

### 2.3.1 Geometric Brownian Motion

The Geometric Brownian Motion is the basis of the *Black-Scholes-Merton* model used to price options and is defined by the following difference equation:

$$dX_t = \mu(t)X_t dt + D(t, X_t)\sigma(t)dB_t, \quad (10)$$

where  $\mu(t)$  indicates the level of return,  $\sigma(t)$  the volatility and  $dB_t$  is a simple Brownian motion. Volatility is deterministic and constant and there are no jumps. Increments are independent on previous states.

### 2.3.2 Fractional Brownian Motion

The *Fractional Brownian Motion* is a long memory process introduced in [30]:

$$B_H(t) = B_H(0) + \frac{1}{\Gamma(H + 1/2)} \left( \int_{-\infty}^0 ((t-s)^{H-1/2} - (-s)^{H-1/2}) dB(s) + \int_0^t (t-s)^{H-1/2} dB(s) \right). \quad (11)$$

It is also referred to as a *self-similar* process. A stochastic process  $X_t$ , with  $t \in \mathbb{R}$ , is said to be self-similar if there exist  $H > 0$  such that for any *scaling factor*  $c > 0$ ,

$$X_{ct} \stackrel{\mathcal{L}}{=} c^H X_t, \quad (12)$$

with  $H$  the Hurst exponent and  $(\stackrel{\mathcal{L}}{=})$  equivalence in distribution. Self-similar processes are stochastic models where a scaling in time is equivalent, *in term of distribution*, to an appropriate scaling in space. Moreover, if, for any  $k$ , the distribution of  $(X_{t_1+c} - X_{t_1+c-1}, \dots, X_{t_k+c} - X_{t_k+c-1})$  does not depend on  $c$ ,  $X_t$  is said to be self-similar with *stationary increments*. So, a Gaussian process  $B_H(t)$  is called a *Fractional Brownian Motion*, if it satisfies: 1.  $B_H(t)$  is self-similar with  $0 < H < 1$ ; 2.  $B_H(t)$  has stationary increments. When  $H = 0.5$  a simple Brownian Motion with independent increments is recovered. When  $0 < H < 0.5$  the *Fractional Brownian Motion* is said to be anti-persistent, which means that increments tend to be opposite signed. Conversely, when  $0.5 < H < 1$  it is said to be persistent, which means that increments tend to be equally signed.

### 2.3.3 Autoregressive Fractionally Integrated Moving Average

The model of an *Autoregressive Fractionally Integrated Moving Average* process (*ARFIMA*) of a time series of order  $(p, d, q)$  with mean  $\mu$ , may be written, using the lag operator  $L$ , as:

$$\Phi(L)(1-L)^d(y_t - \mu) = \Theta(L)\epsilon_t, \quad (13)$$

with  $\epsilon_t$  *i.i.d.* and  $\sim (0, \sigma_\epsilon^2)$ . The autoregressive component of the process is represented by the factor:

$$\Phi(L) = 1 - \phi_1 L - \dots - \phi_p L^p, \quad (14)$$

where the lag operator of order  $p$  shifts the value of  $y_t$  back to  $p$  observations, so that one obtains:

$$\Phi(L)y_t = (1 - \phi_1 L - \dots - \phi_p L^p)y_t = y_t - \phi_1 y_{t-1} - \dots - \phi_p y_{t-p}. \quad (15)$$

The moving average component of the process is represented by the factor:

$$\Theta(L)\epsilon_t = (1 + \theta_1 L + \dots + \theta_q L^q)\epsilon_t = \epsilon_t + \theta_1 \epsilon_{t-1} + \dots + \theta_q \epsilon_{t-q}. \quad (16)$$

The fractionally differencing operator  $(1-L)^d$  is defined as:

$$(1-L)^d = \sum_{n=0}^{\infty} \frac{\Gamma(k-d)L^k}{\Gamma(-d)\Gamma(k+1)}. \quad (17)$$

Note that the process is stationary only for  $-0.5 < d < 0.5$ . For  $d < |0.5|$  the ARFIMA process is said to exhibit long memory.

The power spectral representation  $f(\lambda)$  of Fractional Brownian Motions and Autoregressive Fractionally Integrated Moving Average Processes provides further details regarding their power law behavior and the relation between the characteristic exponents. It is :

$$\begin{aligned} f(\lambda) &\sim |\lambda|^{-2d} && \text{(ARFIMA)} \\ f(\lambda) &\sim |\lambda|^{1-2H} && \text{(FBM)} \end{aligned} \tag{18}$$

yielding:

$$H = d + 1/2 \tag{19}$$

Among financial models, the *autoregressive fractionally integrated moving average* is one of the most common processes used to model prices of long-range correlated assets.

### 3 Results

In this section, the results of the application of the cluster entropy method to several FBM and ARFIMA series are presented. The moving average cluster entropy can be implemented via the MATLAB codes available at the repository [31].

To the purpose to have a set of generic benchmark values for the cluster entropy, first Geometric Brownian Motion series are analysed. Geometric Brownian Motion series are generated by means of the MATLAB tool available at [32]. Several Geometric Brownian Motion processes are analysed with parameters varying in the range  $0 \leq \mu \leq 1 \cdot 10^{-7}$  and  $5 \cdot 10^{-4} \leq \sigma \leq 5 \cdot 10^{-6}$ . Figure 1 reports cluster entropy and market dynamic index results on GBM series with parameters:  $\mu = 1 \cdot 10^{-7}$  and  $\sigma = 5 \cdot 10^{-4}$ .

Results of the cluster entropy approach applied to fractional Brownian motion are reported in Figures 2. The fractional Brownian motion series were generated by means of the FRACLAB tool available at [33]. Several Fractional Brownian Motion series with Hurst exponent varying in the range  $0.1 \leq H \leq 0.9$  are analysed. Figure 2 shows the cluster entropy for time horizon  $M = 1$  and  $M = 12$ , i.e. corresponding respectively to one period of data (one month) and twelve periods of data (one year) for FBM series with  $H = 0.3$ ,  $H = 0.5$  and  $H = 0.8$ .

In general, cluster entropy calculated at different time horizons  $M$  presents a similar behavior. On account of Eq. (7), one can expect power-law correlated clusters with a smooth logarithmic increase of the entropy for  $\tau < n$ . Conversely, for  $\tau \geq n$ , the exponentially correlated decay sets the entropy to increase linearly with the term  $\tau/n$  dominating. However, a quite different behavior is observed for different  $H$ . For  $H = 0.3$  (anti-correlated FBM series) the cluster entropy curves exhibit a very limited dependence on the moving average window  $n$  over the range of investigated  $\tau$ . For  $H = 0.5$  the cluster entropy curves vary more significantly as the moving average window  $n$  changes. For  $H = 0.8$  the cluster entropy curves vary even more remarkably and take increasing values for increasing  $n$ .

The dependence of the cluster entropy on the Hurst exponent  $H$  and the temporal horizon  $M$  is reflected in the results of the Market Dynamic Index  $I(M, n)$  plotted in Figure 3. The Market Dynamic Index  $I(M, n)$  is estimated over several FBM series with different Hurst exponent. For anticorrelated series  $0 \leq H \leq 0.5$   $I(M, n)$  curves overlap for all the moving average windows  $n$  and time horizons  $M$ . For positively correlated series  $0.5 \leq H \leq 0.9$ ,  $I(M, n)$  exhibits slightly different values as a function of time horizons  $M$ . One can also note that the magnitude of the marginal increments in  $I(M, n)$  at large  $n$  increases as  $H$  increases for  $0 \leq H \leq 0.5$ , reaches a maximum for  $H = 0.5$  and then decreases again for  $0.5 \leq H \leq 0.9$ . This effect is evident in the insets of Figure 3.



The cluster entropy analysis is implemented on *Autoregressive Fractionally Integrated Moving Average* (ARFIMA) series obtained by means of simulations for several combination of parameters [34]. The extent of investigated parameters are marked by alphabet labels and are reported in Table 2 for ARFIMA (1,d,1) and in Table 3 for ARFIMA (3,d,2) and ARFIMA(1,d,3).

Cluster entropy results on ARFIMA (1,d,1), are plotted in Figures 4, 5. The corresponding market dynamic indexes  $I(M, n)$  calculated by using the data of the cluster entropy results on ARFIMA (1,d,1) are shown in 6. Cluster entropy results on ARFIMA (3,d,2) and ARFIMA(1,d,3), corresponding to parameters marked by alphabet labels in Table 3, are reported in Figures 7, 8, 9. Market Dynamic Index for series generated by ARFIMA processes are reported in Figure 6. With differencing parameter  $0 < d < 0.2$ , Market Dynamic Index curves are  $n$ -invariant for small values of  $n$ , but horizon dependence emerges at larger  $n$ . When  $0.2 < d < 0.5$  Market Dynamic Index curves show a significant horizon dependence even at small  $n$ . Therefore, according to the choice of the differencing parameter  $d$ , series generated by ARFIMA processes can reproduce the effect shown by the cluster entropy in real-world financial markets.

## 4 Discussion and Conclusions

The cluster entropy behavior described by Equation (7) has been replicated by simulations performed on artificially generated series, with results reported in Section 3. Figures show cluster entropy results for the following processes: Fractional Brownian Motion (Figure 2); Autoregressive Fractionally Integrated Processes (Figures 4, 5, 7, 8). The behavior of cluster entropy curves is well represented by Equation (7), however deviations occur at extreme cases. In general, one can observe that power-law correlated clusters, characterized by length  $\tau < n$ , determine the logarithmic behavior of the entropy, regardless of the moving average window value  $n$ . On the other hand, exponentially correlated clusters, i.e. clusters with length  $\tau \geq n$ , are related to the linear behavior prescribed by the excess entropy term  $\tau/n$ , which depends on the moving average window  $n$  and with slope decreasing as  $1/n$ . The Market Dynamic Index  $I(M, n)$  is deduced from the cluster entropy results by means of Equation (9). Cumulative measures are useful to summarize key information in a single numerical index.  $I(M, n)$  gathers the information present in the sequences at different time horizons  $M$  and moving average windows  $n$ .

The Market Dynamic Index  $I(M, n)$  for series generated by means of Fractional Brownian Motion processes with Hurst exponent  $0 < H < 0.5$  (anticorrelated FBMs) do not present any horizon dependence. Conversely, Fractional Brownian Motion series with  $0.5 < H < 1$  (positively correlated FBMs) do show some horizon dependence. However, as it will be clarified below, Fractional Brownian Motion series fail to fully reproduce the financial markets behavior.

The Market Dynamic Index estimated in long-range positively correlated sequences replicate the characteristic behaviour observed in financial markets [24].

In the case of ARFIMA processes, a significant horizon dependence emerges, as one can note by observing the Market Dynamic indexes plotted in Figures 6 and 9. Thus, cluster entropy for series generated by ARFIMA process exhibit horizon dependence as observed in real world financial markets. The extent of long range dependence and its microscopic origin have been scrutinized in several studies [28, 29] since the introduction of the ARFIMA process.

To further validate our findings a statistical significance test has been performed by using the paired t-test to check the null hypothesis  $h = 0$  that the cluster entropy values obtained by ARFIMA simulations come from distributions with equal mean and same variance with a probability  $p$  with simple Brownian Motion assumed as benchmark

$H = 0.5$  results are reported in Table 4.

We report the results of the  $T$ -paired test performed on NASDAQ, DJIA and S&P500 markets in Table 5 [24]. A qualitative comparison between Table 4 and Table 5 suggests an overall similarity of the ARFIMA and real world markets. In particular, one can note that the  $p$  values in column [f1] are quite close to those of the S&P500 suggesting a correlation degree with Hurst exponent  $H \simeq 0.65$  and differencing parameter  $d \simeq 0.15$  for S&P500. Probability values in column [e2] are close to S&P500, confirming the value  $H \simeq 0.65$  and  $d \simeq 0.15$ . The probability values for DJIA are better approximated by the set of ARFIMA parameters in column [b1] and column [a2] suggesting lower values of the correlation exponents:  $H \simeq 0.55$  and  $d \simeq 0.05$ . The lower values of the probability  $p$  indicate a more complex behavior of the NASDAQ with stronger deviation from the fully uncorrelated Brownian motion. By looking at the Table 4, one can relate the NASDAQ behaviour to higher values of the long-range parameters. In particular, the NASDAQ probability values become closer to parameter sets corresponding to higher correlation degrees [i2] and [n2]. The values of the correlation exponents are expected to increase and reach values  $H \simeq 0.75$  and  $d \simeq 0.25$ .

The cluster entropy behavior appears deeply linked to the positive persistence and long-range correlation. In real-world financial series horizon dependence deviates from the case of absolutely random series, such as those generated by means of stochastic differential equations. The Market Dynamic Index, obtained via an integration performed on cluster entropy, provides this result in a cumulative and, thus, particularly robust form. Moreover, the different horizon dependence of NASDAQ and DJIA, where the former is a diversified stock market with a high degree of heterogeneity and the latter is an index representative of a chosen set of industrial stocks, is consistent with the ability of the cluster entropy index to quantify market heterogeneity. Therefore, contrary to the traditional financial market theories, the hypothesis of efficient markets and rational investor behavior do not hold.

## Funding

Pietro Murialdo acknowledges financial support from FuturICT 2.0 a FLAG-ERA Initiative within the Joint Transnational Calls 2016.

## Conflicts of interest

The authors declare no conflict of interest. The funders had no role in the design of the study; in the collection, analyses, or interpretation of data; in the writing of the manuscript, or in the decision to publish the results.

## References

- [1] P. Grassberger, I. Procaccia, Characterization of strange attractors, *Phys. Rev. Lett.* 50 (5) (1983) 346.
- [2] J. P. Crutchfield, K. Young, Inferring statistical complexity, *Phys. Rev. Lett.* 63 (2) (1989) 105.
- [3] J. P. Crutchfield, Between order and chaos, *Nature Physics* 8 (1) (2012) 17–24.
- [4] M. Ormos, D. Zibriczky, Entropy-based financial asset pricing, *PLoS ONE* 9 (12) (2014) e115742.
- [5] J. Yang, Information theoretic approaches in economics, *Journal of Economic Surveys* 32 (3) (2018) 940–960.
- [6] A. Ghosh, C. Julliard, A. P. Taylor, What Is the Consumption-CAPM Missing? An Information-Theoretic Framework for the Analysis of Asset Pricing Models, *Review of Financial Studies* 30 (2) (2017) 442–504. doi:{10.1093/rfs/hhw075}.
- [7] D. Backus, M. Chernov, S. Zin, Sources of entropy in representative agent models, *The Journal of Finance* 69 (1) (2014) 51–99.
- [8] R. Zhou, R. Cai, G. Tong, Applications of entropy in finance: A review, *Entropy* 15 (11) (2013) 4909–4931.
- [9] C. R. Shalizi, K. L. Shalizi, R. Haslinger, Quantifying self-organization with optimal predictors, *Physical review letters* 93 (11) (2004) 118701.
- [10] A. Carbone, G. Castelli, H. E. Stanley, Analysis of clusters formed by the moving average of a long-range correlated time series, *Phys. Rev. E* 69 (2004) 026105.
- [11] A. Carbone, H. E. Stanley, Scaling properties and entropy of long-range correlated time series, *Physica A: Statistical Mechanics and its Applications* 384 (1) (2007) 21–24.
- [12] A. Carbone, Information measure for long-range correlated sequences: the case of the 24 human chromosomes, *Scientific Reports* 3 (2013) 2721.
- [13] X. Zhao, Y. Sun, X. Li, P. Shang, Multiscale transfer entropy: Measuring information transfer on multiple time scales, *Communications in Nonlinear Science and Numerical Simulation* 62 (2018) 202–212.
- [14] A. Humeau-Heurtier, The multiscale entropy algorithm and its variants: A review, *Entropy* 17 (5) (2015) 3110–3123.

- [15] H. Niu, J. Wang, Quantifying complexity of financial short-term time series by composite multiscale entropy measure, *Communications in Nonlinear Science and Numerical Simulation* 22 (1-3) (2015) 375–382.
- [16] C. E. Shannon, A mathematical theory of communication, part i, part ii, *Bell Syst. Tech. J.* 27 (1948) 623–656.
- [17] A. N. Kolmogorov, Three approaches to the quantitative definition of information', *Problems of information transmission* 1 (1) (1965) 1–7.
- [18] M. Li, P. Vitányi, et al., *An introduction to Kolmogorov complexity and its applications*, Vol. 3, Springer, 2008.
- [19] E. Marcon, I. Scotti, B. Hérault, V. Rossi, G. Lang, Generalization of the partitioning of shannon diversity, *PLoS ONE* 9 (3) (2014) e90289.
- [20] N. Rubido, C. Grebogi, M. S. Baptista, Entropy-based generating markov partitions for complex systems, *Chaos: An Interdisciplinary Journal of Nonlinear Science* 28 (3) (2018) 033611.
- [21] G. A. Darbellay, I. Vajda, Estimation of the information by an adaptive partitioning of the observation space, *IEEE Transactions on Information Theory* 45 (4) (1999) 1315–1321.
- [22] R. Steuer, L. Molgedey, W. Ebeling, M. A. Jimenez-Montaña, Entropy and optimal partition for data analysis, *The European Physical Journal B-Condensed Matter and Complex Systems* 19 (2) (2001) 265–269.
- [23] L. Ponta, A. Carbone, Information measure for financial time series: Quantifying short-term market heterogeneity, *Physica A: Statistical Mechanics and its Applications* 510 (2018) 132 – 144.  
URL <http://www.sciencedirect.com/science/article/pii/S0378437118308100>
- [24] L. Ponta, A. Carbone, Anna, Quantifying horizon dependence of asset prices: a cluster entropy approach, *arXiv* (2019).
- [25] J. E. Vera-Valdés, On long memory origins and forecast horizons, *Journal of Forecasting* (2020).
- [26] T. Graves, C. L. Franzke, N. W. Watkins, R. B. Gramacy, E. Tindale, Systematic inference of the long-range dependence and heavy-tail distribution parameters of arfima models, *Physica A: Statistical Mechanics and its Applications* 473 (2017) 60–71.
- [27] R. P. D. Bhattacharyya, Ranajoy, The dynamics of india's major exchange rates, *Global Business Review* (2020).
- [28] G. Bhardwaj, N. Swanson, An empirical investigation of the usefulness of arfima models for predicting macroeconomic and financial time series, *Journal of Econometrics* 131 (1-2) (2006) 539–578.  
URL <https://www.scopus.com/inward/record.uri?eid=2-s2.0-33644532899&doi=10.1016%2Fj.jeconom.2005.01.016&partnerID=40&md5=367dd4f6fb200763e83b4490719d36fc>

- [29] R. T. Baillie, C. Kongcharoen, G. Kapetanios, Prediction from arfima models: Comparisons between mle and semiparametric estimation procedures, *International Journal of Forecasting* 28 (1) (2012) 46 – 53.  
URL <http://www.sciencedirect.com/science/article/pii/S0169207011000380>
- [30] B. B. Mandelbrot, J. W. Van Ness, Fractional Brownian Motions, Fractional Noises and Applications, *SIAM Review* 10 (4) (1968) 422–437, publisher: Society for Industrial and Applied Mathematics.  
URL [www.jstor.org/stable/2027184](http://www.jstor.org/stable/2027184)
- [31] Moving average cluster entropy code, [https://www.dropbox.com/sh/9pfeltf2ks0ewj1/AACjuScK\\_gZxmyQ\\_mDFmGHoya?dl=0](https://www.dropbox.com/sh/9pfeltf2ks0ewj1/AACjuScK_gZxmyQ_mDFmGHoya?dl=0).
- [32] Geometric brownian motion code, <https://it.mathworks.com/help/finance/gbm.html>.
- [33] Fractional brownian motion code, <https://project.inria.fr/fraclab/>.
- [34] Autoregressive fractional integrated moving average code, <https://www.mathworks.com/matlabcentral/fileexchange/25611-arfima-simulations>.

$M$	$N$	$N_M$	$t_S$	$t_S^*$
1	586866	586866	1.0000	1
2	1117840	586866	1.9048	1
3	1704706	586866	2.9048	2
4	2291572	586866	3.9048	3
5	2906384	586866	4.9524	4
6	3493250	586866	5.9524	5
7	4069315	586866	6.9340	6
8	4712062	586866	8.0292	8
9	5243029	586866	8.9339	8
10	5885781	586866	10.0292	10
11	6461845	586866	11.0108	11
12	6982017	586866	11.8971	11

**Table 1.** Example of cumulative series. Lengths for each time horizon  $M$  are reported for NASDAQ data in 2018. Each row corresponds to the number of transactions that took place in month  $M$  in 2018 plus the number of transactions that occurred in past months of 2018. These lengths are used as a reference to generate artificial series and allow a correct comparison between results obtained on real and artificial data.

$H$	$d$	$\phi$	$\theta$	
0.55	0.05	0.20	0.90	a1
		0.90	0.20	b1
0.60	0.10	0.20	0.90	c1
		0.90	0.20	d1
0.65	0.15	0.20	0.90	e1
		0.90	0.20	f1
0.70	0.20	0.20	0.90	g1
		0.90	0.20	h1
0.75	0.25	0.20	0.90	i1
		0.30	0.40	j1
		0.85	0.85	k1
		0.20	0.20	l1
		0.90	0.40	m1
		0.85	0.85	n1
0.80	0.30	0.20	0.90	o1
		0.90	0.20	p1
0.98	0.48	0.30	0.40	q1
		0.85	0.85	r1
		0.90	0.40	s1
		0.85	0.85	t1

**Table 2.** Full set of parameter range for the ARFIMA (1,d,1) processes simulated in this work. Specifically  $H$  is the Hurst exponent and  $d$  is the differencing parameter (1<sup>st</sup> and 2<sup>nd</sup> columns) which are related by Equation (20),  $\phi$  is the autoregressive parameter (3<sup>rd</sup> column), and  $\theta$  is the moving average parameter (4<sup>th</sup> column).

$H$	$d$	$\phi_1$	$\phi_2$	$\phi_3$	$\theta_1$	$\theta_2$	$\theta_3$	
0.55	0.05	0.20	-	-	0.90	0.90	0.90	a2
		0.90	0.90	0.90	0.20	0.20	-	b2
0.60	0.10	0.20	-	-	0.90	0.90	0.90	c2
		0.90	0.90	0.90	0.20	0.20	-	d2
0.65	0.15	0.20	-	-	0.90	0.90	0.90	e2
		0.90	0.90	0.90	0.20	0.20	-	f2
0.70	0.20	0.20	-	-	0.90	0.90	0.90	g2
		0.90	0.90	0.90	0.20	0.20	-	h2
0.75	0.25	0.20	-	-	0.90	0.90	0.90	i2
		0.90	0.90	0.90	0.20	0.20	-	j2
0.80	0.30	0.20	-	-	0.90	0.90	0.90	k2
		0.40	0.16	-	0.90	0.81	0.73	l2
		0.90	0.90	0.90	0.20	0.20	-	m2
0.85	0.35	0.20	-	-	0.90	0.90	0.90	n2
0.98	0.48	0.40	0.16	-	0.90	0.81	0.73	o2

**Table 3.** Full set of parameter range for ARFIMA (3,d,2) and ARFIMA(1,d,3) processes simulated in this work. Specifically  $H$  is the Hurst exponent and  $d$  is the differencing parameter which are related by Equation (20) (1<sup>st</sup> and 2<sup>nd</sup> columns);  $\phi_1$ ,  $\phi_2$  and  $\phi_3$  are the autoregressive parameters (3<sup>rd</sup>, 4<sup>th</sup> and 5<sup>th</sup> columns);  $\theta_1$ ,  $\theta_2$  and  $\theta_3$  are the moving average parameters (6<sup>th</sup>, 7<sup>th</sup> and 8<sup>th</sup> columns).

$M$	$[b1]$	$[f1]$	$[l1]$	$[a2]$	$[e2]$	$[i2]$	$[n2]$	$[o2]$
1	0.9597	0.7938	0.6013	0.8519	0.6779	0.4956	0.3542	0.2314
2	0.9863	0.8429	0.6985	0.9293	0.7883	0.6566	0.5414	0.4304
3	0.982	0.8789	0.7743	0.938	0.8346	0.7362	0.6468	0.5576
4	0.9848	0.8922	0.8031	0.956	0.8689	0.7827	0.7147	0.638
5	0.9878	0.9062	0.8325	0.9608	0.8809	0.8102	0.7528	0.6911
6	0.994	0.9197	0.8517	0.9724	0.9043	0.8417	0.784	0.7322
7	0.9785	0.9186	0.8633	0.9617	0.9038	0.8521	0.8036	0.7614
8	0.993	0.9321	0.8775	0.9762	0.9229	0.871	0.8333	0.7931
9	0.9867	0.937	0.889	0.9737	0.9273	0.8809	0.8438	0.8100
10	0.9813	0.9333	0.8952	0.971	0.9261	0.8880	0.8533	0.8195
11	0.9816	0.9436	0.9011	0.9749	0.9326	0.8965	0.8643	0.8342
12	0.9853	0.9451	0.9072	0.9741	0.9353	0.9019	0.8764	0.8508

**Table 4.** Probability  $p$  to reject the null hypothesis that the cluster entropy values for the ARFIMA processes at varying horizons  $M$ , have same mean and variance of the Fractional Brownian Motion with  $H = 0.5$ . The probability  $p$  has been estimated by standard  $T$ -paired test. First column reports the temporal horizon  $M$ . The other columns refers to parameter sets  $[b1]$ ,  $[f1]$ ,  $[l1]$ ,  $[a2]$ ,  $[e2]$ ,  $[i2]$ ,  $[n2]$ ,  $[o2]$  of Table 2 and Table 3.

$M$	NASDAQ	S&P500	DJIA
1	0.5154	0.7399	0.8892
2	0.6026	0.8335	0.9257
3	0.647	0.8588	0.9332
4	0.6631	0.8814	0.9283
5	0.6823	0.9018	0.9417
6	0.7124	0.9246	0.9534
7	0.7162	0.9224	0.9461
8	0.7288	0.9309	0.9618
9	0.7370	0.9479	0.9645

**Table 5.** Probability  $p$  to reject the null hypothesis that the cluster entropy values for the NASDAQ, DJIA and S&P500 at varying horizons  $M$  have same mean and variance of the Fractional Brownian Motion with  $H = 0.5$ . First column reports the temporal horizon  $M$ . The probability  $p$  has been estimated by standard  $T$ -paired test [24]



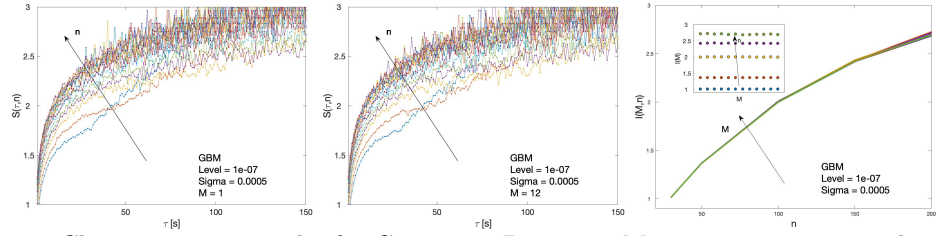


**Fig 1.** Cluster entropy results for Geometric Brownian Motion series, generated with following parameters:  $\mu = 1 \cdot 10^{-7}$  and  $\sigma = 5 \cdot 10^{-4}$  (left and middle). The market dynamic index  $I(M, n)$  is also shown (right). One can note that  $I(M, n)$  is practically independent on the temporal horizon  $M$ .

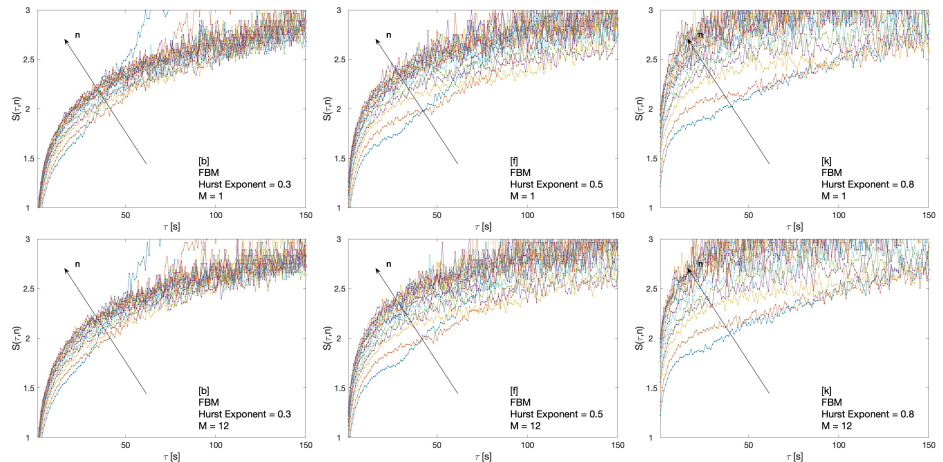


**Fig 2.** Cluster entropy results curves for Fractional Brownian Motion (FBM) series with  $H = 0.3$ ,  $H = 0.5$ ,  $H = 0.8$ . First row shows results for time horizon  $M = 1$  (approximately equivalent to the first month (January 2018) of raw data for NASDAQ, S&P500, DIJA). The second row shows results for time horizon  $M = 12$  (approximately equivalent to twelve months of data in NASDAQ, S&P500, DIJA, i.e the whole 2018 year).

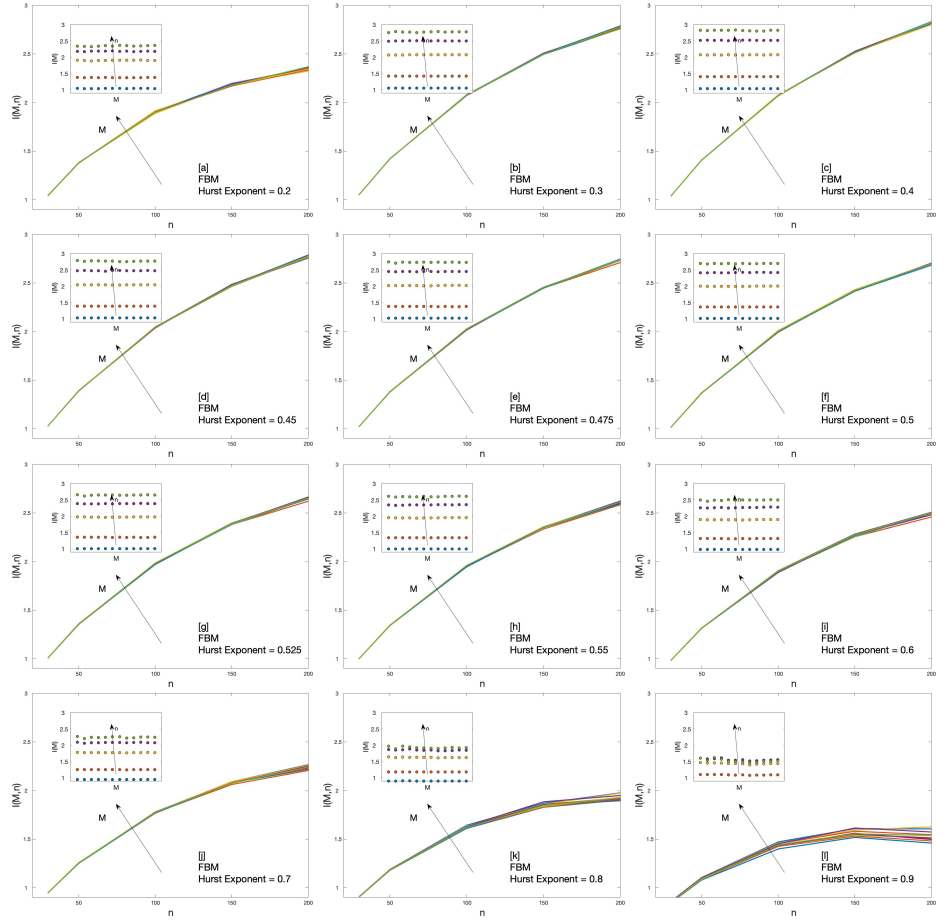


**Fig 3.** Market Dynamic Index  $I(M, n)$  for Fractional Brownian Motion series with Hurst exponent ranging from  $H = 0.2$  to  $H = 0.9$  respectively from (a) to (l).

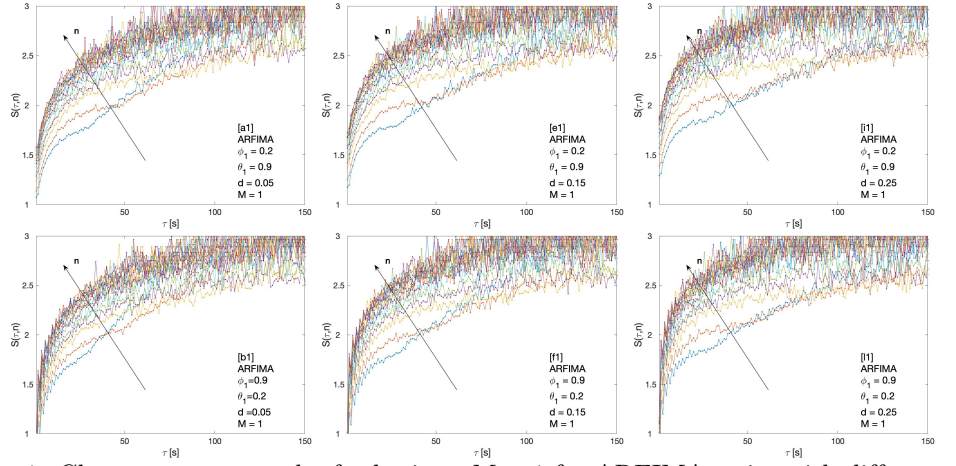


**Fig 4.** Cluster entropy results for horizon  $M = 1$  for ARFIMA series with different combinations of the differencing parameter  $d$ , autoregressive parameter  $\phi$  and moving average parameter  $\theta$ . The differencing parameter takes values  $d = 0.05$ ,  $d = 0.15$ ,  $d = 0.25$  with a different combinations of autoregressive and moving average parameter. The full set of analysed values of  $d$ ,  $\phi$  and  $\theta$  is reported in Table 2.

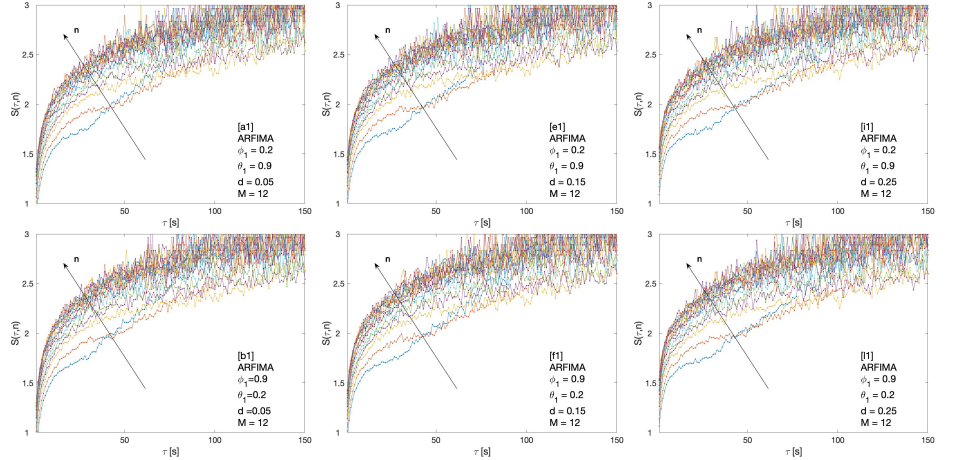


**Fig 5.** Cluster entropy results for horizon  $M = 12$  on ARFIMA series with different combinations of the differencing parameter  $d$ , autoregressive parameter  $\phi$  and moving average parameter  $\theta$ . The differencing parameter takes values  $d = 0.05$ ,  $d = 0.15$  and  $d = 0.25$  with a different combination of autoregressive and moving average parameters. The full set of analysed values of  $d$ ,  $\phi$  and  $\theta$  is reported in Table 2.

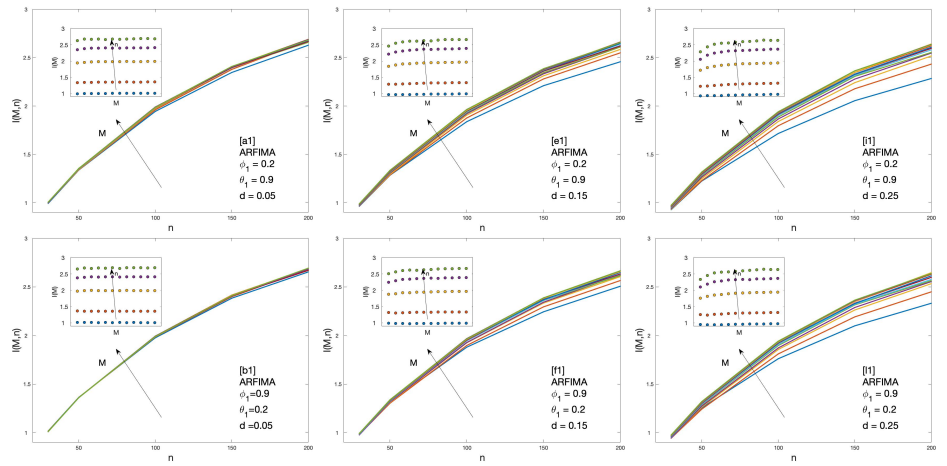


**Fig 6.** Market Dynamic Index  $I(M, n)$  for ARFIMA series with different combinations of the differencing parameter  $d$ , autoregressive parameter  $\phi$ , and moving average parameter  $\theta$ . The differencing parameter takes values  $d = 0.05$ ,  $d = 0.15$ ,  $d = 0.25$ , with a different combination of autoregressive and moving average parameters. The full set of analysed values of  $d$ ,  $\phi$  and  $\theta$  is reported in Table 2

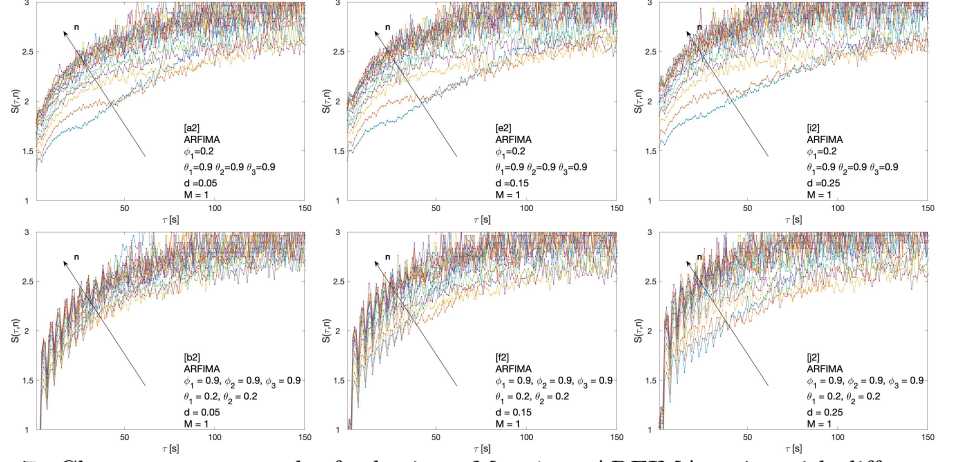


**Fig 7.** Cluster entropy results for horizon  $M = 1$  on ARFIMA series with different combinations of the differencing parameter  $d$ , autoregressive parameter  $\phi_1$ ,  $\phi_2$ , and  $\phi_3$  and moving average parameter  $\theta_1$ ,  $\theta_2$  and  $\theta_3$ . The differencing parameter takes values  $d = 0.05$ ,  $d = 0.15$ ,  $d = 0.25$ , with a different combination of autoregressive and moving average parameters. The full set of analysed values of  $d$ ,  $\phi$  and  $\theta$  is reported in Table 3.

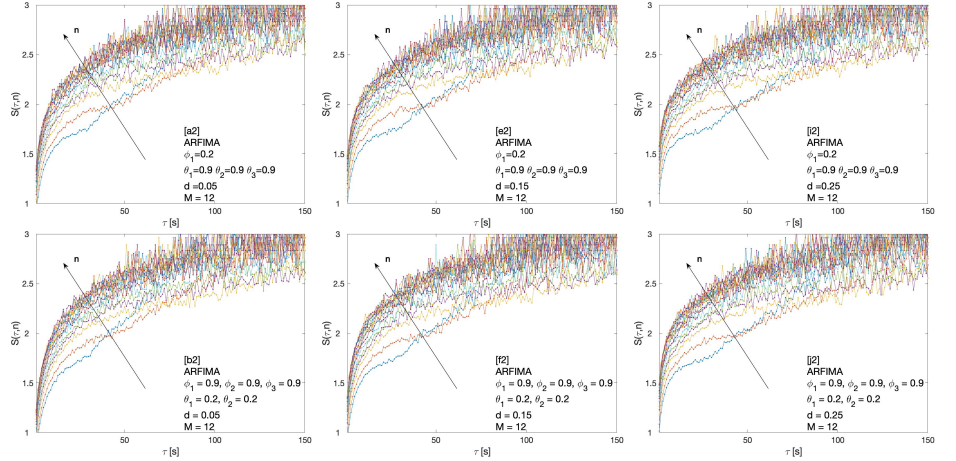


**Fig 8.** Cluster entropy results for horizon  $M = 12$  on ARFIMA series with different combinations of the differencing parameter  $d$ , autoregressive parameter  $\phi_1$ ,  $\phi_2$ , and  $\phi_3$  and moving average parameter  $\theta_1$ ,  $\theta_2$  and  $\theta_3$ . The differencing parameter takes values  $d = 0.05$ ,  $d = 0.15$  and  $d = 0.25$ , with a different combination of autoregressive and moving average parameters. The full set of analysed values of  $d$ ,  $\phi$  and  $\theta$  is reported in Table 3.

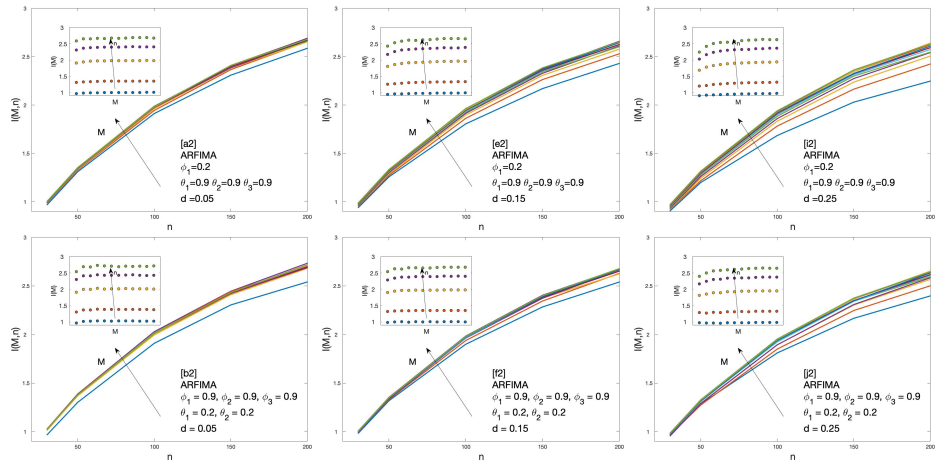


**Fig 9.** Market Dynamic Index  $I(M, n)$  for ARFIMA series with different combinations of the differencing parameter  $d$ , autoregressive parameter  $\phi_1$ ,  $\phi_2$ , and  $\phi_3$  and moving average parameter  $\theta_1$ ,  $\theta_2$  and  $\theta_3$ . The differencing parameter takes values  $d = 0.05$ ,  $d = 0.15$  and  $d = 0.25$ , with a different combination of autoregressive and moving average parameters as reported in Table 3.